[논 문] 한국재료학회지
Korean Journal of Materials Research
Vol. 11, No. 3 (2001)

사파이어(α-Al_2O_3) 단결정에 있어 basal slip (0001)1/3<11$\bar{2}$0>전위 Part I: 전위속도

윤석영 · 이종영
부산대학교 생산기술연구소, 특별연구원

Basal slip (0001)1/3<11$\bar{2}$0> dislocation in sapphire (α-Al_2O_3) single crystals Part I: Dislocation velocity

Seog-Young Yoon and Jong-Young Lee
Special researcher, Research Institute of Industrial Technology, Pusan National University
30 Changjeon-dong, Keumjeong-ku, Pusan 609-735, Korea

(2001년 1월 6일 받음, 2001년 2월 12일 최종수정본 받음)

초 록 사파이어 (α-Al_2O_3) 단결정에 있어 basal slip (0001)1/3<11$\bar{2}$0>의 전위속도를 4점 곡강도를 이용하여 측정하였다. 이 곡강도는 온도 1200℃ 에서 1400℃ 그리고 응력은 90MPa, 120MPa, 150MPa에서 행하여졌다. 전위속도는 4 점굽힘 시편의 굽힘변위속도에 의해 구하여졌다. 얻어진 전위속도를 이용하여 전위속도의 온도 및 응력 의존성에 대해 검토하였다. 전위속도의 온도의존성을 이용하여 basal slip 전위속도를 위한 활성화에너지를 구하였으며, 그 값은 대략 2.2±0.4eV이었다. 한편, 전위속도의 응력의존성을 나타내는 응력지수 m은 2.0±0.2이었다.

Abstract The basal slip (0001)1/3<11$\bar{2}$0> dislocation velocity in sapphire (α-Al_2O_3) single crystals was measured by four-point bending test. The bending experiment was carried out in the temperature range from 1200℃ to 1400℃ at various engineering stresses 90MPa, 120MPa, and 150MPa. The velocity of such dislocations was estimated from the bending displacement rate of the four-point bend sample. The dependence of temperature and stress in dislocation velocity was investigated. The activation energy for dislocation velocity was determined to be about 2.2±0.4eV. In addition, the stress exponent (m) describing the stress dependence of dislocation velocities was in the range of 2.0±0.2.

Key words: sapphire single crystals, basal slip, dislocation velocity.

1. Introduction

Sapphire has thermodynamic stability and relatively high melting point so that makes it a promising candidate for use as a structural material in oxidizing environment, and for single crystal fiber reinforcements in advanced composite ceramics. The mechanical properties of sapphire (α-Al_2O_3) single crystals have been studied extensively after Kronberg[1] predicted that slip and twinning to be important modes of plastic deformation mechanism of sapphire at elevated temperatures. A number of investigators[2~10] have determined the primary slip systems at high temperatures[2~5], work-hardening and dynamic recovery[6~9], and creep.[10]

In recent years, microhardness studies, which has been shown to be useful to investigate the deformation behavior of brittle materials, have been used to study the micro-plastic behavior around microhardness indents at room temperature[11,12] and at high temperatures.[13~15] It has been shown that dislocation plasticity can occur even at roon temperature and that the slip systems varied with temperature.

It is generally accepted the dislocation velocity and density of mobile dislocations are important parameters describing plastic deformation in crystalline solids. Johnston and Gilman[16] first measured the dislocation velocity in lithium fluoride (LiF) single crystals to understand details of the micromechanism of plasticity. Since then, the dislocation velocity under different conditions has been studied in metals, ionic crystals, and semiconductors [see Nadgonyi review book[17]]. However, because of the difficult experimental conditions required for dislocation velocity measurements in ceramics (the need for high stresses and high temperature) the measurements of the dislocation velocity in single crystals of structural ceramics are very limited.[18,19]

To understand the microscopic aspects of the plastic deformation in sapphire single crystals, it is of fundamental interest to measure the dislocation velocity as a function of temperature and resolved shear stress.

Therefore, the aim of the present paper is to investigate the basal slip dislocation velocity using the 4-point bending test in the temeprature range from 1200℃ to 1400℃ at various engineering stresses 90MPa, 120MPa, and 150MPa.

2. Experimental procedure

High-purity ingots of Czochralski-grown undoped sapphire single crystals [Union Carbide Co.] with very low grown-in dislocation densities ($<10^2 cm^{-2}$) were used for this study. Specimens ($25\times3\times1.5mm^3$) suitable for 4-point bending were oriented using the Laue back-reflection X-ray techniques and cut using a Bueher isomet diamond saw. One sample (Type A) had face parallel to $(11\bar{2}3)$ with the long axis of the 4-point sample parallel to $[\bar{2}111]$. The other sample (Type B) had one face parallel to $(11\bar{2}0)$ with the long axis of the 4-point sample parallel to $[\bar{8}80\bar{5}]$ as shown in Fig. 1. Four sides of the specimen were polished using 30㎛, 15㎛, and 3㎛ diamond pastes, down to 1㎛ and syton (the colloidal silica) as a final step.

Dislocations were introduced on the $(11\bar{2}0)$ and $(11\bar{2}3)$ respective sample faces using a Vickers diamond indentor mounted in a hot hardness tester (Model QM, Nikon, Inc.) and an atmosphere of 10^{-5} torr vacuum with 0.5N load using a dwell time of 15sec at 1000 ℃. An array of indents was made on both the tensile and compressive faces of the four-point bend sample. To reveal the dislocation substructure around the indentation site the indented surfaces were etched in saturated solution of KOH between 380℃ and 400℃ for 10-15 min.

After indentation, the 4-point bend sample was subjected to a static load in the Ar atmosphere in material testing machine (MTS System Co.) using bending jigs made from high quality sintered SiC. The temperature was controlled using a thermocouple mounted near the sample and was maintained constant within ±2℃.

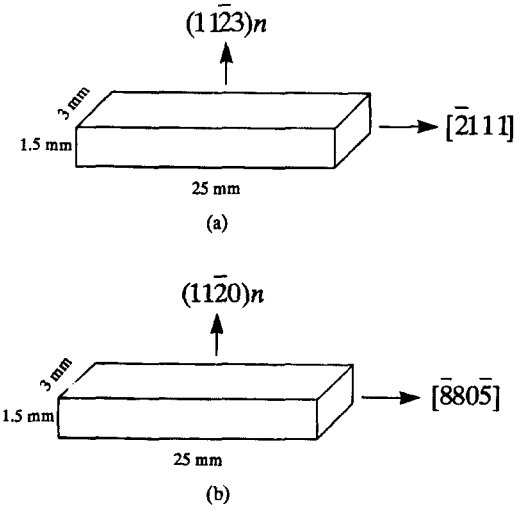

Fig. 1. Specimen orientation for measuring the basal slip dislocation velocity : (a) type A $(11\bar{2}3)$ plane and (b) type B $(11\bar{2}0)$.

Fig. 2. Optical micrograph of etched pattern on the type A $(11\bar{2}3)$ sample surface after indentation (R : rhombohedral twinning, B : basal slip dislocation).

3. Results and discussion

3.1 Indented structures

3.1.1 $(11\bar{2}3)$ specimen

As can be seen in Fig. 2, basal plane dislocations were generated in the vicinity of indentations on the $(11\bar{2}3)$ surface at elevated temperatures around an indent (1000℃, 0.5N, and 15sec). The indented substructure is quite complex in that they contain deformation twins (rhombohedral twins) as well as the basal slip dislocations. However, the type A specimen fractured prior to plastic deformation during 4-point bending. The reason for this can be explained assuming self-climb dissociation of stationary basal slip dislocation. As can be seen in Fig. 3, basal slip dislocations have been shown to dissociate by self-climb. This is believed to be due to the fact that the basal plane has high stacking fault energy ($\sim2.1J/m^2$) in comparison with the prism plane ($\sim0.2J/m^2$).[20,21] In order to combine the two partial dislocations as shown in Fig. 3, one or both partial dislocations need to move (climb). However, one of the partial dislocations on the prism plane has a very low Schmid factor (~0.24) [see Table 1]. Thus, the samples fractured before the partial dislocations could recombine to from a glissile basal dislocation. As a result, the type A specimens were not appropriate for measurements of the basal slip dislocation velocity.

3.1.2. $(11\bar{2}0)$ specimen

The etched structure around an indent on a

Table 1. Calculated Schmid-factors on the $(11\bar{2}3)$ plane sample and the loading direction $[\bar{2}111]$.

Slip plane	Slip direction	m(Schmid factor)
(0001)	$1/3\,[2\bar{1}\bar{1}0]$	0.5
(0001)	$1/3\,[\bar{1}2\bar{1}0]$	0.25
(0001)	$1/3\,[\bar{1}\bar{1}20]$	0.25

On partials
$1/3[2\bar{1}\bar{1}0]$ $1/3\,[1\bar{1}00]+1/3\,[\bar{1}0\bar{1}0]$

Dissociation plane	Partials	m(Schmid factor)
$(2\bar{1}\bar{1}0)$	$1/3\,[10\bar{1}0]$	0.24
	$1/3\,[1\bar{1}00]$	0.24
	$1/3\,[01\bar{1}0]$	0

Table 2. Calculated Schmid-factors on the $(11\bar{2}0)$ plane sample and the loading direction $[\bar{8}80\bar{5}]$.

Slip plane	Slip direction	m(Schmid factor)
(0001)	$1/3\,[\bar{2}110]$	0.43
(0001)	$1/3\,[1\bar{2}10]$	0.43
(0001)	$1/3\,[11\bar{2}0]$	0.25

On partials
$1/3[\bar{2}110]$ $1/3\,[\bar{1}100]+1/3\,[\bar{1}010]$

Dissociation plane	Partials	m(Schmid factor)
$(2\bar{1}\bar{1}0)$	$1/3\,[10\bar{1}0]$	0.22
	$1/3\,[1\bar{1}00]$	0.44
	$1/3\,[01\bar{1}0]$	0.22

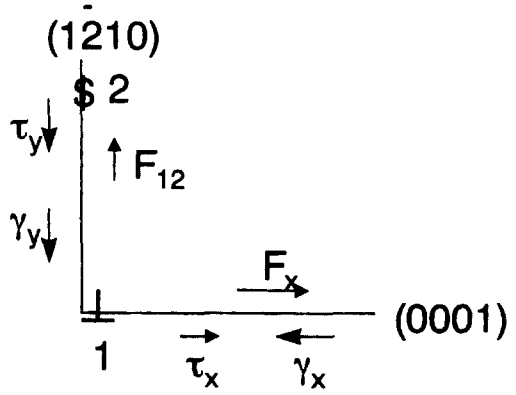

Fig. 3. Schematic diagram of two dislocations after self-climb dissociated partials on basal slip dislocation. 1 : edge dislocation, 2 : screw dislocation, stacking fault energy : γ_x=2.1J/m², γ_y=0.17J/m² : respectively.

Fig. 4. Optical micrograph of etched pattern on the type B $(11\bar{2}0)$ sample surface after indentation(R : rhombohedral twinning, B : basal slip dislocation).

$(11\bar{2}0)$ plane surface made at elevated temperature (1000℃, 0.5N and 15sec) is shown in Fig. 4. The indented structure show the presence of deformation twins (rhombohedral twin) as well as basal slip dislocations similar to the deformation substructure observed

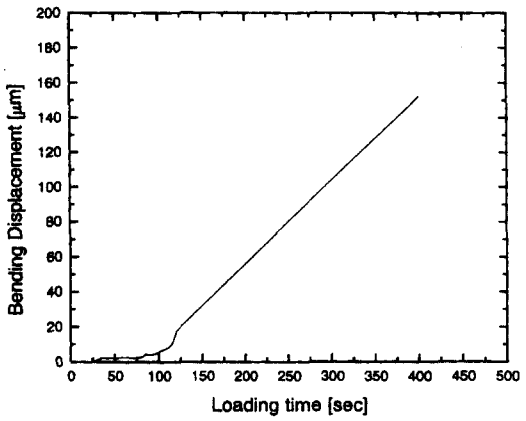

Fig. 5. Typical bending displacement on the type B$(11\bar{2}0)$ sample as a function of loading time at given conditions : 90MPa applied stress at 1350℃.

in $(11\bar{2}3)$ plane specimens. However, the type B specimen could be deformed during 4-point bending even though the basal dislocations may have been dissociated via self-climb. This is because the Schmid factor for a partial dislocation on prism plane (~0.43) is higher than in case of the type A $(11\bar{2}3)$ samples (~0.24) [see Table 2]. Thus, during the application of a stress, the basal plane dislocation can recombine prior to fracture, and $(11\bar{2}0)$ samples proved to be suitable for bending displacement experiments to estimate of the basal slip dislocation velocity.

3.2 Bending displacement as a function of temperature and stress

As mentioned above, the$(11\bar{2}0)$ type specimen was used for bending displacement test for estimating the basal slip dislocation velocity. Fig. 5 shows the typical bending displacement rate as a function of time at constant shear stress (120MPa). The applied stress was calculated using the equation given by Timosenko[22] for beams in 4-point bending, the outer fiber stress (σ) is

Table 3. The strain rate determined by the bending displacement rate experiments at various temperatures and stresses.

Applied stress	1200℃	1250℃	1300℃	1350℃	1400℃
90MPa	0.00012 ±0.00003		0.042 ±0.0012	0.014 ±0.0025	
120MPa	0.0035 ±0.0002	0.0102 ±0.0007	0.032 ±0.0027	0.068 ±0.0031	0.123 ±0.013
150MPa	0.025 ±0.0024		0.173 ±0.014	0.235 ±0.027	

given by

$$\sigma=\frac{3P(L-l)}{2wh^2} \quad (1)$$

where P is the applied load, w is the specimen width, h is the specimen thickness, L is the separation of the outer supports and l is the separation of the inner supports. Of interest, as shown by Fig. 5, is the fact that an incubation time was needed before the bending displacement (a macroscopic plasticity) occurred. During the experiments at different temperatures, it was shown that the incubation time decreased with increasing temperature. In particularly, there was no (or very short) incubation time at 1400℃. In addition, the bending displacement rates were increased as the temperature increased.

3.3. Dislocation velocity

The dislocation velocity is related to the macroscopic strain rate through the Orowan equation

$$d\varepsilon/dt=\rho bV \quad (2)$$

where $d\varepsilon/dt$ is the strain rate, ρ is the density of mobile dislocation, b is the magnitude of the Burger's vector and V is the average dislocation velocity. The dislocation density and strain rate should be obtained in order to calculate the dislocation velocity. First of all, the strain rate ($d\varepsilon/dt$) can be calculated from the bending displacement rate ($d\delta/dt$) as the following relationship which is given by[22]

$$\frac{d\delta}{dt}=A\frac{d\varepsilon}{dt} \quad (3)$$

where A is a constant which includes the specimen thickness and Young' modulus. The strain rate at various temperatures and stresses are shown in Table 3.

On the other hand, to estimate an average dislocation velocity from the strain rate using the Orowan equation[23], the dislocation density must also be known. Thus, the dislocation density was measured using TEM

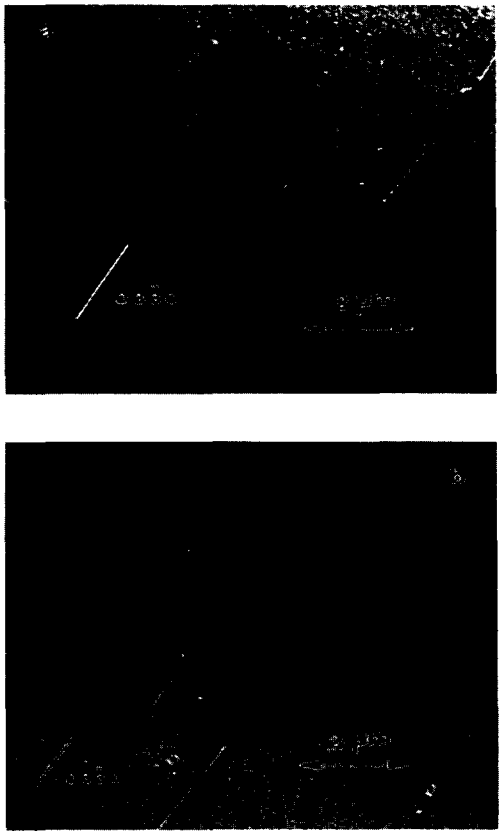

Fig. 6. TEM micrographs [weak beam dark field image g = (0330] for measuring the dislocation density at different temperatures: (a) 1200℃ and (b) 1250℃.

micrographs of the deformed samples. The TEM images were taken from representative regions of each specimen, with the majority of the dislocations clearly resolvable as shown in Fig. 6. A cross-grid of lines was then drawn on each micrograph. The total projected length of dislocations was derived from the number of intercepts with the two sets of parallel lines, using the expression derived by Smith and Guttman.[24] The average dislocation density, ρ_v, was calculated by the following equation:

$$\rho_v=[(n_1/L_1)+(n_2/L_2)]/t \quad (4)$$

where n_1 and n_2 are the average number of intersec

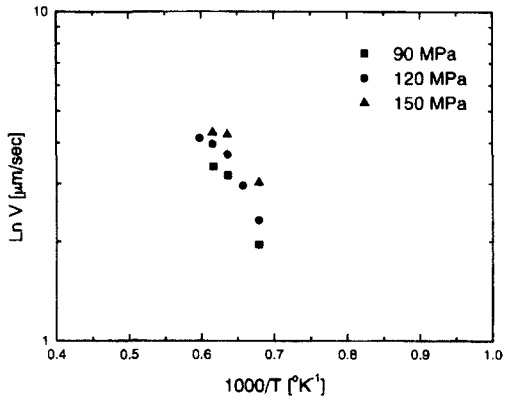

Fig. 7. Temperarture dependence of basal slip dislocation velocity at different applied stresses.

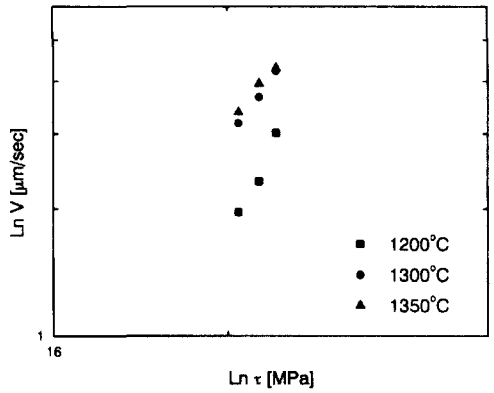

Fig. 8. Stress dependence of basal slip dislocation velocity at various temperatures.

tions of dislocation lines with the two sets of grid lines, L_1 and L_2 are the total lengths of the two sets of grid lines, t is the thickness of the foil. Using experimentally obtained strain rate and dislocation density, the dislocation velocity was calculated as a function of temperature at different stresses.

To obtain the activation energy, the values of log (velocity) plotted against (1/T) are shown in Fig. 7. The respective stresses at which the measurements were made are also indicated. At constant stress the dislocation velocity as a function of temperature obeys the relation in equation (5),

$$V = V_0 \exp\left[-\frac{U}{kT}\right] \tag{5}$$

where V_0 is a function of stress, k is the Boltzmann constant, and U is the activation energy for the basal slip dislocation velocity. The activation energies (U) were obtained from the slope of the least square curve fit through the data points with equation (5). In our experimental temperature range, the activation energy can be estimated to be 2.2±0.4eV in the range of temperature from 1200 to 1400℃. These values are lower than the activation energy for prism plane slip dislocation (3.8±0.2eV).[25] Therefore, basal slip has a lower thermal activation energy than prism plane slip in the experimental temperature (1200-1400℃), which is consistent with the fact that basal slip is the easy slip system above 700℃.[26]

In order to estimate the stress dependence on the dislocation velocity, the bending experiments were carried out in the range 60MPa, 120MPa and 150MPa at different temperatures (1200℃, 1300℃ and 1350℃). The results are shown in Fig.8. These results appear silimar to those of Johnston and Gilman[16], in that the logarithm of velocity varies linearly with the logarithm of the applied stress. The relationship between velocity and stress shown in Fig.8 can be written in the form:

$$V = A\left[\frac{\tau}{\tau_0}\right]^m \tag{6}$$

where A is constant, m is the stress exponent, and τ_0 is a reference stress for dimensional correctness. The values of stress exponent (m) was determined to be 2.0±0.2.

4. Conclusions

The basal slip dislocation velocity in sapphire single crystals was measured by 4-point bending experiment. Under optimum conditions, it is suggested that the basal slip dislocation velocity could be measured using the bending on prism plane specimen. An incubation time was needed for the basal slip dislocations to glide. The activation energy for basal slip dislocation velocity was around 2.2±0.4eV in the range of temperature from 1200 to 1400℃. The stress exponent (m) for basal slip dislocation velocities was 2.0±0.2.

References

1. M.L. Kronberg, *Acta Metall.*, **5** [9], 507 (1957).
2. D.J. Gooch and G.W. Groves, *Acta Metall.*, **55** [2], 105 (1972).
3. J.B. Wachtman and L.H. Maxwell, *J. Am. Ceram. Soc.*, **40**, 377 (1957).
4. R. Scheupein and P. Gibbs, *J. Am. Ceram. Soc.*, **43** [9], 458-72 (1960).
5. J.D. Snow and A.H. Heuer, *J. Am. Ceram. Soc.*, **56** [3], 153 (1973).
6. J. Cadoz, J. Castaing, D.S. Phillips and A.H. Heuer, *Acta Metall.*, **30**, pp. 2205-2218 (1982).

7. B.J. Pletka, T.E. Mitchell, and A.H. Heuer, *J. Am. Ceram. Soc.*, **57**[9], 388 (1974).
8. B.J. Pletka, A.H. Heuer and T.E. Mitchell, *Acta Metall.*, **25**, 25 (1977).
9. B.J. Pletka, T.E. Mitchell, and A.H. Heuer, *Acta Metall.*, **30**, 147-56 (1982).
10. R. Chang, *J. Appl. Phys.*, **31**[3], 484-487 (1960).
11. B.J. Hockey, "*Deformation of ceramic materials*", Edited by R.C. Bradt and R.E. Tressler. Plenum, New York, 1975.
12. H.M. Chan and B.R. Lawn, *J. Am. Ceram. Soc.*, **71**[1], 29 (1988).
13. W. Kollenberg, *J. Mater. Sci.* **23** (1988).
14. B.Ya. Farber, S.Y. Yoon, K.P.D. Lagerlöf and A. H. Heuer, *Zeitschr. fur Metallkunde,* Vol.26, 426-429 (1993).
15. B.Ya. Farber, S.Y. Yoon, K.P.D. Lagerlöf and A. H. Heuer, *Phys. Stat. Sol. (a) [137], 485-498 (1993).*
16. *W.G. Johnston and J.J. Gilman, J. Appl. Phys.*, **30**[2], 129-44 (1959).
17. E. Nadgornyi, "*Dislocation dynamics and mechanical properties of crystals*", in Progress in Materials Science, (ed. J.W. Christian, P. Haasen, and T.B. Massalski), Permagon Press, (1988).
18. B.Ya. Farber, A.S. Chiarelli and A.H. Heuer, *Phil. Mag.* **A 70**[1], 201-17 (1994).
19. Hyung-Sun Kim and Steve Roberts, *J. Am. Ceram. Soc.*, **77**[12], 3099-104 (1994).
20. D.G. Howitt and T.E. Mitchell, *Phil. Mag.* **A, 44**[1], 229-38 (1981).
21. P.R. Kenway, *Phil. Mag.*, B, **68**[2], 171-83 (1993).
22. S. Timoshenko, "*Theory of Elasticity*", pp. 391 (McGrow-Hill) (1961).
23. J.P. Hirth and J. Lothe, "*Theory of Dislocations*", pp. 679 (New York: McGraw-Hill) (1972).
24. C.S. Smith and L. Guttman, *Trans. Amer. Inst. Mining, Met. Petrol. Eng.* **197** (1953).
25. S.Y. Yoon and J.Y. Lee, *J. Korean Association of Crystal Growth,* **10**[4], 337-343 (2000).
26. K.P.D. Lagerlöf, A.H. Heuer and T.E. Mitchell., *J. Am. Ceram. Soc.*, **77**[2], 385-97 (1994).